Geometric nonlinear analysis of tensioned membranes using the Positional Finite Element Method

Christian L. Perlin[1], Humberto B. Coda[1]

[1]*Department of Structural Engineering, São Carlos School of Engineering, University of São Paulo*
Av. Trabalhador Sãocarlense, 400, 13566-590, São Carlos, SP, Brazil
christianperlin@usp.br, hbcoda@sc.usp.br

Abstract. This paper describes a total Lagrangian formulation of the Finite Element Method based on positions and its application to the analysis of tensioned membranes. In these structures, the geometric nonlinearity is very pronounced due to large displacements and the lack of flexural stiffness of the elements; therefore, the equilibrium must be evaluated at the current configuration and the geometric stiffness plays an important role in the analysis. The use of nodal positions as main variables allows a direct consideration of the geometric nonlinearity. For the positional description of membrane elements, two mappings are employed: one for the initial configuration and other for the current configuration, resulting in a simple chain rule to calculate the deformation gradient. These mappings are defined in such a way that results in square and invertible mapping gradients for the membrane element in three-dimensional space. In the form finding stage, the dynamic relaxation technique is employed to find an initial prestressed configuration for further loaded analysis. Numerical examples for isotropic fabrics are presented to demonstrate the applicability of the positional formulation in the assessment of stiffness and displacements in this category of problems.

Keywords: Membrane structures, Geometric nonlinearity, Positional finite element method

1 Introduction

Membranes are used as structural elements in various fields such as construction, industry and engineering. In buildings, they are commonly employed in the covering of large span areas, having some desirable characteristics as low self-weight, prefabrication and sustainability features. Besides, the smooth curved shapes of this system draw attention for its architectural beauty.

Despite that advantages, the structural analysis of membranes is a challenging task. The elements lack compressive and flexural stiffness, allowing only tensile stresses. As a consequence, the structure undergo large displacements and it is needed to evaluate the equilibrium at the displaced configuration, that is, the problem is geometrically nonlinear. Because of these complexities, robust numerical methods such the Finite Element Method (FEM) are commonly used (Tabarrok and Qin [1], Bonet et al. [2]). Moreover, the form of the structure cannot be imposed and must be calculated to obtain a configuration in equilibrium only under tensile stresses, a process known as form finding (Tabarrok and Qin [1]; Barnes [3]; Pauletti and Pimenta [4]).

In this paper, we developed an alternative formulation of the Finite Element Method for the application in the analysis of tensioned membrane structures. The employed formulation, namely Positional Finite Element Method, considers a total Lagrangian description obtained from the principle of stationary potential energy and uses the nodal positions as variables, instead of displacements as in the classical approach, naturally ensuring the consideration of the geometric nonlinearity. The Positional FEM was presented by Coda [5] after the article of Bonet et al. [2] and other works explored its functionalities in several problems (Greco et al. [6]; Coda and Paccola [7]; Soares et al. [8]). Relatively to applications in tensioned structures, Coda et al. [9] used the formulation in the analysis of cable structures and Kan et al. [10] applied the method in the study of tensegrities. The present work expands the borders to cover the analysis of three-dimensional membrane elements.

2 Formulation

In order to use the principle of stationary potential energy, the derivative of the strain energy stored in the elements must be calculated and it is function of the strains and stresses developed. The Positional Finite Element Method obtains the strains from the initial and current mappings from a dimensionless space, using a total Lagrangian description with the Green-Lagrange strain $\boldsymbol{E}$ and the second Piola-Kirchhoff stress $\boldsymbol{S}$ as measures.

2.1 Membrane element kinematics

The membrane element is considered as acting in plane stress state, so it is necessary to adopt local axes for the definition of the thickness direction in space. Although the membrane element is a surface (two-dimensional), we considered it as a false solid, in which only the mid-surface is modeled and the displacements and stresses in the normal direction has constant values. That is in accordance with the plane stress state consideration and allows a consistent definition of the mappings from a dimensionless space $\xi_1\xi_2\xi_3$, depicted in Fig. 1. With mapping gradients $\boldsymbol{A^0}$ and $\boldsymbol{A^1}$ for the initial and current configurations, respectively, the gradient $\boldsymbol{A}$ of the deformation function $\vec{f}$ can be expressed as:

$$\boldsymbol{A} = \boldsymbol{A^1} \cdot \left(\boldsymbol{A^0}\right)^{-1}. \tag{1}$$

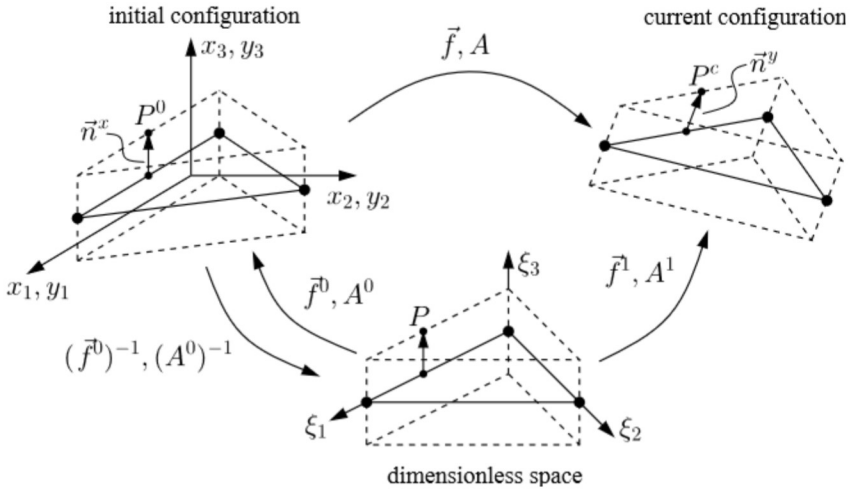

Figure 1. Configuration mappings and deformation function

Local coordinates are defined such that x_3 is normal to the mid-surface in the integration point and x_1 and x_2 are tangent, forming an orthonormal basis. Then, the mapping of the initial configuration (point P^0) is given by:

$$\vec{f}^0\left(\xi_1, \xi_2, \xi_3\right) = x_i = X_i^\alpha \phi^\alpha\left(\xi_1, \xi_2\right) + t\xi_3 n_i^x, \tag{2}$$

in which X_i^α are the initial coordinates of node α in direction i, ϕ^α is the value of the shape function related to node α, considered as a Lagrange polynomial, t is the thickness of the element and n_i^x is the component i of the normal unitary vector in the initial configuration. Similarly, the mapping of the current configuration (point P^c) is:

$$\vec{f}^1\left(\xi_1, \xi_2, \xi_3\right) = y_i = Y_i^\alpha \phi^\alpha\left(\xi_1, \xi_2\right) + t\xi_3 n_i^y, \tag{3}$$

where y indicates the corresponding current quantities. We remark that the normal vector $\vec{n}^y$ is different from $\vec{n}^x$ for large displacements and the derivatives of this vector must be calculated carefully.

It can be demonstrated that the thickness t does not influences the components of the tensor $\boldsymbol{A}$, so it will be considered $t = 1$. Also, $\xi_3 = 0$ in the mid-surface. Then, the mapping gradients can be calculated by:

$$\boldsymbol{A}^0 = \begin{bmatrix} X_1^\alpha \phi_{,1}^\alpha & X_1^\alpha \phi_{,2}^\alpha & 0 \\ X_2^\alpha \phi_{,1}^\alpha & X_2^\alpha \phi_{,2}^\alpha & 0 \\ 0 & 0 & 1 \end{bmatrix} \quad \text{and} \quad \boldsymbol{A}^1 = \begin{bmatrix} Y_1^\alpha \phi_{,1}^\alpha & Y_1^\alpha \phi_{,2}^\alpha & n_1^y \\ Y_2^\alpha \phi_{,1}^\alpha & Y_2^\alpha \phi_{,2}^\alpha & n_2^y \\ Y_3^\alpha \phi_{,1}^\alpha & Y_3^\alpha \phi_{,2}^\alpha & n_3^y \end{bmatrix}. \tag{4}$$

These gradients are square and invertible, allowing the direct use of eq. (1). Once the deformation gradient has been calculated, the Green-Lagrange strain is obtained by:

$$\boldsymbol{E} = \frac{1}{2}\left(\boldsymbol{A}^t \cdot \boldsymbol{A} - \boldsymbol{I}\right), \tag{5}$$

where $\boldsymbol{I}$ is the identity tensor.

The Saint-Venant-Kirchhoff constitutive model was adopted, determining a linear relation between strains $\boldsymbol{E}$ and stresses $\boldsymbol{S}$ through a constitutive tensor $\mathbb{C}$ that is the same used in the classical Hooke's Law:

$$\boldsymbol{S} = \mathbb{C} : \boldsymbol{E}. \tag{6}$$

The second Piola-Kirchhoff stress $\boldsymbol{S}$ can be related to the Cauchy stress $\boldsymbol{\sigma}$ by:

$$\boldsymbol{\sigma} = \frac{1}{\det(\boldsymbol{A})} \boldsymbol{A} \cdot \boldsymbol{S} \cdot \boldsymbol{A}^t. \tag{7}$$

2.2 Equilibrium equations and nonlinear system solution

According to the principle of stationary potential energy, the system is at equilibrium when the first variation of the total potential energy Π is zero. In this work, we have $\Pi = P + U$, where P is the potential of external applied forces, considered here as conservatives, and U is the strain energy stored in the elements. The equilibrium is evaluated as:

$$\delta\Pi = \delta P + \delta U = \left(\frac{\partial P}{\partial \vec{Y}} + \frac{\partial U}{\partial \vec{Y}}\right) \delta\vec{Y} = 0 \quad \therefore \quad \frac{\partial \Pi}{\partial \vec{Y}} = \frac{\partial P}{\partial \vec{Y}} + \frac{\partial U}{\partial \vec{Y}} = \vec{0}, \tag{8}$$

with δ denoting variation and $\vec{Y}$ being the vector of current nodal positions.

The derivative of P is the negative nodal values of external applied forces, which can be comprised of volume forces, surface tractions and concentrated loads. The derivative of U is an internal force vector given by:

$$\frac{\partial U}{\partial \vec{Y}} = \vec{F}^{int} = \int_{V_0} \boldsymbol{S} : \frac{\partial \boldsymbol{E}}{\partial \vec{Y}} \, dV_0, \tag{9}$$

Equation 8 is a nonlinear system of equations due to the dependence between the nonlinear strain $\boldsymbol{E}$ (function of positions) with the internal force. Using the Newton-Raphson method in the solution, eq. (8) is rewritten as:

$$\vec{G}\left(\vec{Y}\right) = -\vec{F}^{ext} + \vec{F}^{int} = \vec{0}, \tag{10}$$

where $\vec{G}$ is an unbalanced force vector, equals to zero in an exact solution. The solution is obtained iteratively by:

$$\boldsymbol{H} \cdot \Delta\vec{Y} = -\vec{G}\left(\vec{Y}^0\right), \tag{11}$$

where $\boldsymbol{H}$ is the Hessian matrix of the system, given by the derivative of the force vector $\vec{G}$, $\vec{Y}^0$ is a first solution attempt and $\Delta\vec{Y}$ is the correction in the nodal positions.

The procedure stops when the correction becomes small according a tolerance tol defined by the user, which was evaluated as:

$$\frac{\|\Delta\vec{Y}\|}{\|\vec{X}\|} \leq tol. \tag{12}$$

When only conservative forces are considered, the derivative of $\vec{F}^{ext}$ regarding positions is zero. Therefore, the Hessian matrix consists only in the derivative of $\vec{F}^{int}$ given by eq. (9):

$$\boldsymbol{H} = \int_{V_0} \frac{\partial \boldsymbol{S}}{\partial \vec{Y}} : \frac{\partial \boldsymbol{E}}{\partial \vec{Y}} + \boldsymbol{S} : \frac{\partial^2 \boldsymbol{E}}{\partial \vec{Y} \otimes \partial \vec{Y}} \; dV_0. \tag{13}$$

The first term of eq. (13) is the elastic stiffness, which depends on the geometry and the constitutive model. The second term, which appears only in the geometric nonlinear formulation, is called geometric stiffness and is particularly important in the analysis of membrane structures due to the low elastic stiffness of the elements. Because the geometric stiffness is proportional to the stress $\boldsymbol{S}$ developed, the prescription of a prestress state increases the stiffness of the elements and is a common practice in cable and membrane structures.

2.3 Form finding

The shape of a rigid structure, like beams or trusses, is a known parameter at the beginning of load analysis stage. However, in membrane structures, because geometry and load interacts allowing only tensile stresses in the elements, form choice is not as free as for rigid structures and a precise description of geometry is not available. The process of calculating this initial form in equilibrium is named *form finding*. Many equilibrium configurations are possible, related to the boundary conditions and different prestress states that can be imposed to the membrane. The surface of minimum area that covers a boundary is called *minimal surface* and is associated to a uniform isotropic stress.

A wide variety of form finding methodologies can be found in literature. The procedure used in this paper, the dynamic relaxation method, consists in a pseudo-dynamic step-by-step analysis with diagonal mass and stiffness matrices (this last considering only the geometric stiffness). From an arbitrary initial geometry with prescribed stresses, a static equilibrium configuration is obtained at the end of the motion analysis due to an artificial damping. As only the final positions are of interest, parameters such as mass and time step can be chosen conveniently to improve the convergence of the numerical procedure. More detailed information about this method can be found in the works of Barnes [3] and Lewis [11]. Here, we used the formulation with kinetic damping considering:

$$K_i = \Sigma\left(\frac{T}{L}\right)_m \qquad M_i = 50K_i\Delta t^2 \qquad \Delta t = 1, \tag{14}$$

where K_i and M_i are stiffness and mass coefficients for node i, T and L are tension forces and lengths in the membrane element representation for the m links connected to node i and Δt is the time step. This value of M_i was adopted for better convergence.

3 Numerical examples

Two numerical examples are presented to demonstrate the applicability of the proposed formulation in the analysis of membrane structures. The first example illustrates the importance of prestress and geometric stiffness in this class of problems. The second example explores a classic form, the catenoid, in some load cases. In both examples, the membrane has thickness $t = 0.03$ mm and the material considered has elastic modulus $\mathbb{E} = 200$ MPa and Poisson coefficient $\nu = 0.3$. The tolerance used in the Newton-Raphson solution was $tol = 10^{-6}$.

3.1 Example 1: horizontal membrane under vertical load

In this example, a square horizontal membrane with sides of 8.0 m under a vertical load of 100 N/m^2 is analyzed. The four borders are restrained and the mesh is composed of 2048 triangular finite elements with linear interpolation. Displacements and principal stresses were evaluated for two cases: (1) uniform isotropic prestress of 10.0 MPa; (2) without prestress (slack membrane). For a better understanding of the problem, vertical displacements for the prestressed case are shown in Fig. 2. Values for the slack case have a similar pattern.

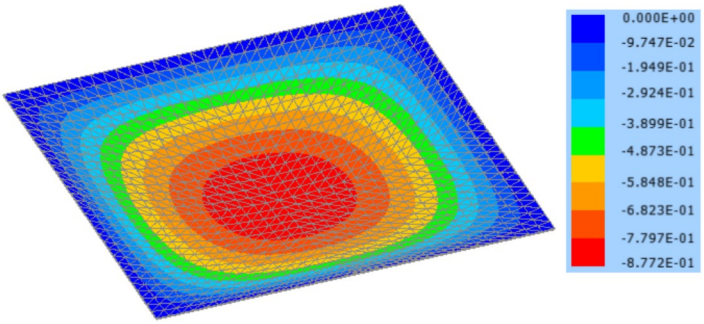

Figure 2. Vertical displacements for the prestressed case (values in m)

The Hessian matrix in the first iteration of the slack case is singular, as the horizontal slack membrane lacks vertical stiffness. To overcome this issue, instead of using a form finding procedure (like the dynamic relaxation), the analysis was simply initiated from the final displaced configuration obtained in the prestressed case, eliminating the prestress and tracing the new equilibrium configuration.

Results of vertical displacements and first principal stresses at a mid-span profile along a vertical plane are displayed in Fig. 3. As expected, the prestress increases the stiffness of the membrane, reducing the maximum displacement from 1.1743 m to 0.8772 m (25.3% reduction). The principal stresses are higher for the prestressed case, but the difference is lower than the value of prestress applied. At the middle of the border, stress in the prestressed membrane is 21.69 MPa, against 18.91 MPa in the slack (2.78 MPa or 14.7% higher). At the center, values are 17.81 MPa in the prestressed membrane and 13.36 MPa in the slack (4.45 MPa or 33.3% higher). These results illustrates the importance of the geometric stiffness in the analysis of membrane structures and its correct evaluation by using the proposed formulation.

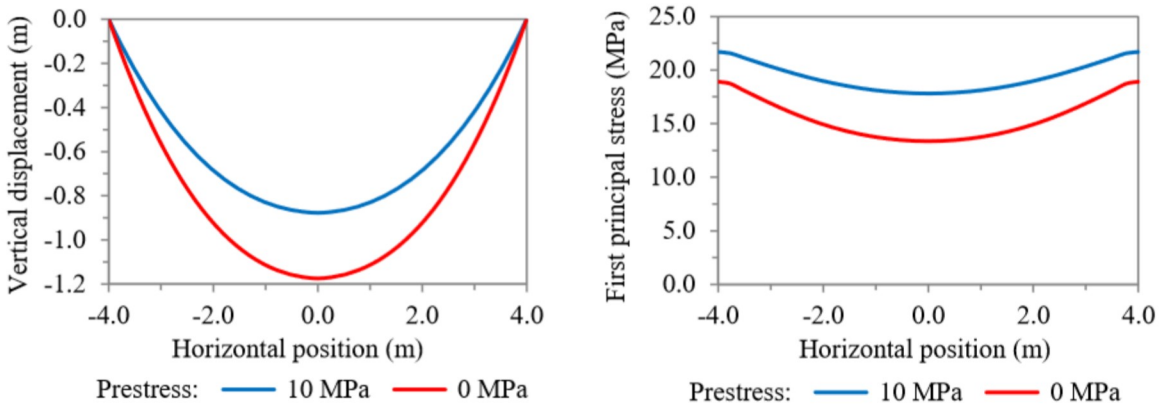

Figure 3. Profile at mid-span: (a) vertical displacements and (b) first principal stresses

3.2 Example 2: catenoid

The catenoid is a surface formed by the revolution of a catenary around an axis. This shape is a classical problem, specially in association to the form finding, as the catenoid shape is one of the few minimal surfaces that

can be analytically described.

In the form finding stage, the mesh used is initially planar, composed of 800 triangular finite elements, with inner ring radius of 4.0 m and outer ring radius of 10.0 m. The inner ring is subjected to a vertical prescribed displacement of 6.0 m and a fictitious isotropic prestress state of 10.0 MPa was considered in the entire membrane, without self-weight. Then, the dynamic relaxation method with kinetic damping was used to obtain the initial configuration in equilibrium for the load analysis stage, depicted in Fig. 4.

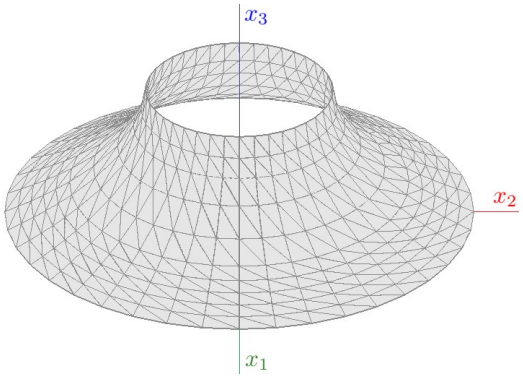

Figure 4. Initial mesh of the catenoid obtained with the form finding procedure

Two load cases were analyzed, both considering the membrane in a slack state (zero prestress): (1) the effect of a horizontal distributed load of 50.0 N/m^2 in the x_2 direction, acting on the left half of the catenoid, subjected also to a vertical load of 0.003 N/m^2 representing self-weight; (2) a vertical elevation of the inner ring of 1.0 m.

For the first load case, displacements in x_2 direction and the first principal stresses are shown in Fig. 5. To avoid compressive stresses in the membrane, a simple wrinkling algorithm was used, considering only non-negative principal stresses (negative principal stresses were set to zero). It can be seen that the horizontal load had little influence in the right half of the catenoid, which remains supporting only the self-weight without compression. On the other hand, the left half develops high tensile stresses to support the horizontal load. This behavior is in accordance to the expected, as an element without compressive stiffness was adopted.

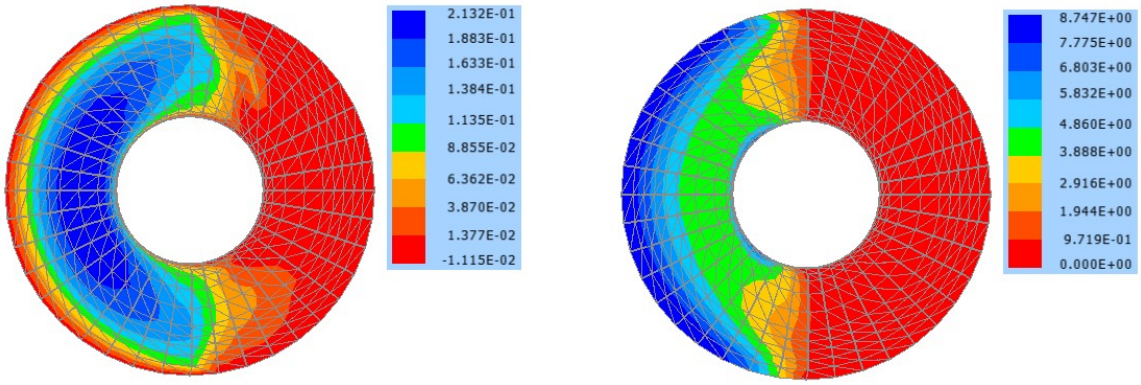

(a) (b)

Figure 5. Catenoid under self-weight and horizontal load: (a) displacements in x_2 direction (in m) and (b) first principal stresses (in MPa)

The inner ring elevation of the second load case was divided into 5 equal steps of 0.2 m each. This elevation may simulate a real prestressing operation on a structure, although it results in a prestress state that is not isotropic. Values of principal stresses are shown in Fig. 6. The first principal stress has, approximately, a linear variation, decreasing with the distance to the center and almost constant for the elevation of 0.2 m. For the second principal stress, the maximum value occurs at some distance of the inner ring, but the variation is still approximately linear from the maximum to the inner and outer borders.

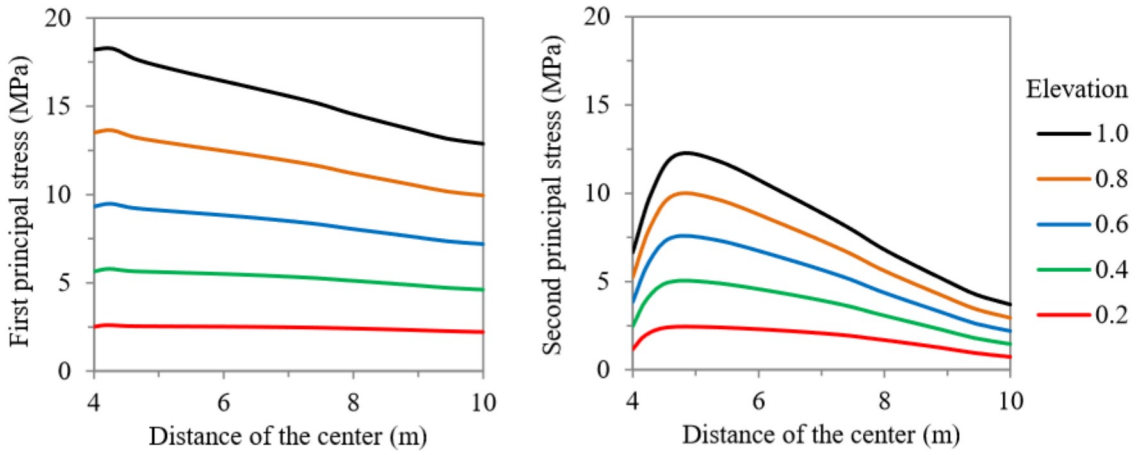

Figure 6. Catenoid under inner ring elevation: principal stresses

4 Conclusions

In this paper, a finite element formulation based on positions was used in the analysis of tensioned membranes. This positional formulation is intrinsically geometric nonlinear and able to evaluate large displacements and geometric stiffness, which are important topics for this kind of structures. The membrane element are considered as a false solid, resulting in square and invertible mapping gradients and allowing an easy calculation of the deformation gradient by a chain rule. Two numerical examples are presented to demonstrate the robustness and simplicity of the numerical procedure. Future implementations will consider more complex constitutive relations, such as orthotropy and plasticity.

Authorship statement. The authors hereby confirm that they are the sole liable persons responsible for the authorship of this work, and that all material that has been herein included as part of the present paper is either the property (and authorship) of the authors, or has the permission of the owners to be included here.

References

[1] B. Tabarrok and Z. Qin. Nonlinear analysis of tension structures. *Computers & Structures*, vol. 45, n. 5, pp. 973–984, 1992.
[2] J. Bonet, R. Wood, J. Mahaney, and P. Heywood. Finite element analysis of air supported membrane structures. *Computer Methods in Applied Mechanics and Engineering*, vol. 190, n. 5, pp. 579–595, 2000.
[3] M. R. Barnes. Form finding and analysis of tension structures by dynamic relaxation. *International Journal of Space Structures*, vol. 14, n. 2, pp. 89–104, 1999.
[4] R. M. O. Pauletti and P. M. Pimenta. The natural force density method for the shape finding of taut structures. *Computer Methods in Applied Mechanics and Engineering*, vol. 197, n. 49, pp. 4419–4428, 2008.
[5] H. B. Coda. An exact FEM geometric non-linear analysis of frames based on position description. In *17th International Congress of Mechanical Engineering (COBEM 2003)*, 2003.
[6] M. Greco, F. A. R. Gesualdo, W. S. Venturini, and H. B. Coda. Nonlinear positional formulation for space truss analysis. *Finite Elements in Analysis and Design*, vol. 42, n. 12, pp. 1079–1086, 2006.
[7] H. B. Coda and R. R. Paccola. Unconstrained finite element for geometrical nonlinear dynamics of shells. *Mathematical Problems in Engineering*, vol. 2009, pp. 1–32, 2009.
[8] H. B. Soares, R. R. Paccola, and H. B. Coda. Unconstrained vector positional shell FEM formulation applied to thin-walled members instability analysis. *Thin-Walled Structures*, vol. 136, pp. 246–257, 2019.
[9] H. B. Coda, A. P. O. Silva, and R. R. Paccola. Alternative active nonlinear total Lagrangian truss finite element applied to the analysis of cable nets and long span suspension bridges. *Latin American Journal of Solids and Structures*, vol. 17, n. 3, 2020.
[10] Z. Kan, H. Peng, and B. Chen. Complementarity framework for nonlinear analysis of tensegrity structures with slack cables. *AIAA Journal*, vol. 56, n. 12, pp. 5013–5027, 2018.
[11] W. J. Lewis. *Tension structures: Form and behaviour*. ICE Publishing, London, 2018.